Author Manuscript

Author Manuscript

Author Manuscript

Author Manuscript

HHS Public Access

Author manuscript

Am J Transplant. Author manuscript; available in PMC 2021 August 27.

Published in final edited form as:

Am J Transplant. 2015 March ; 15(3): 606–617. doi:10.1111/ajt.13007.

Optimization of Intrabone Delivery of Hematopoietic Progenitor Cells in a Swine Model Using Cell Radiolabeling with [89]zirconium

J. M. Pantin[1,2], **R. F. Hoyt Jr.**[3,4], **O. Aras**[5], **N. Sato**[6], **M. Y. Chen**[7], **T. Hunt**[3], **R. Clevenger**[3], **P. Eclarinal**[8], **S. Adler**[8], **P. Choyke**[6,†], **R. W. Childs**[2,*,†]

[1]Division of Hematology and Medical Oncology, Georgia Regents University, Augusta, GA

[2]Hematology Branch, National Heart, Lung and Blood Institute, National Institutes of Health, Bethesda, MD

[3]Laboratory of Animal Medicine and Surgery, National Heart, Lung and Blood Institute, National Institutes of Health, Bethesda, MD

[4]Laboratory Animal Sciences Program, Leidos Biomedical Research, Inc., Frederick National Laboratory, Frederick

[5]Imaging Sciences Training Program, Diagnostic Radiology Department, Warren Magnuson Clinical Center, National Institutes of Health, Bethesda, MD

[6]Molecular Imaging Program, Center for Cancer Research, National Cancer Institute, National Institutes of Health, Bethesda, MD

[7]Advanced Cardiovascular Imaging Laboratory, Cardiovascular and Pulmonary Branch, National Heart, Lung and Blood Institute, National Institutes of Health, Bethesda, MD

[8]Leidos Biomedical Research, Inc., Reston, VA

Abstract

Intrabone (IB) hematopoietic cell transplantation (HCT) of umbilical cord blood in humans remains experimental and the technique has not been optimized. It is unknown whether hematopoietic progenitor cells (HPCs) injected IB are initially retained in the marrow or rapidly enter into the venous circulation before homing to the marrow. To develop an IB-injection technique that maximizes HPC marrow-retention, we tracked radiolabeled human HPCs following

*Corresponding author: Richard W. Childs, childsr@nih.gov.

Authors' Contributions

J.P., R.H. and R.C. wrote the animal study protocol. J.P., T.H., R.C., R.H. and O.A. performed all the animal experiments. O.A., N.S. and P.C. optimized the cell-labeling technique. M.C. performed and analyzed CT imaging. P.E., O. A., S.A.and P.C. performed and analyzed PET imaging. J.-P., T.H., R.H. and R.C. were involved in hardware design and instrumentation. All authors performed experiments. J.-P., O.A., R.H., N.S., P.E., P.C. and R.C. wrote the paper.

†Both senior authors contributed equally to this manuscript as part of an NIH trans-institute collaboration.

Disclosure

The authors of this manuscript have no conflicts of interest to disclose as described by the *American Journal of Transplantation*. Provisional patent applications have been filed for both the ^{89}Zr cell-labeling method and the design of an IB-injection needle for simultaneous intra-marrow pressure measurement with feedback infusion rate-control.

Supporting Information

Additional Supporting Information may be found in the online version of this article.

Author Manuscript Author Manuscript Author Manuscript Author Manuscript

IB-injection into swine. We developed a method to radionuclide-label HPCs using a long-lived positron emitter ^{89}Zr and protamine sulfate that resulted in cellular-retention of low-dose radioactivity. This approach achieved radioactivity levels sufficient for detection by positron emission tomography with both high sensitivity and spatial resolution when fused with computed tomography. We found that conditions utilized in pilot IB-HCT clinical trials conducted by others led to both rapid drainage into the central venous circulation and cellular extravasation into surrounding muscle and soft tissues. By optimizing the needle design, using continuous real-time intra-marrow pressure monitoring, and by reducing the infusion-volume and infusion-rate, we overcame this limitation and achieved high retention of HPCs in the marrow. This method of IB cellular delivery is readily applicable in the clinic and could be utilized in future investigational IB-HCT trials aimed at maximizing marrow retention of HPCs.

Introduction

Although UCB HCT can cure patients with advanced hematological malignancies, graft failure remains a major cause of mortality that impedes the wider applicability of this transplant approach in adults. Recent preclinical animal data and pilot clinical trials suggest IB-HCT may improve engraftment in adult recipients of UCB HCT compared to those receiving conventional IV injection of UCB. Impediments to the progress of IB-HCT include uncertainty regarding injection techniques that optimize the retention of HPCs in the BM. Currently it remains unknown whether IB-injected HPCs in humans are initially retained in the BM or rather rapidly enter into venous circulation before homing back to the BM. Surprisingly, pilot trials in humans were initiated before preclinical studies were developed to optimize techniques of IB-HCT. Preclinical studies require labeling HPCs in a fashion that would allow them to be tracked *in vivo* following IB-injection to provide information necessary to develop an injection technique that maximizes cellular-retention in the BM.

Although ^{111}In oxine traditionally has been used to label HPCs, this approach exposes cells to high doses of radiation which may limit their viability (1) and function (2) *in vivo*. Moreover, images are suboptimal because ^{111}In is a single-photon emitter detected with SPECT cameras, which have limited resolution and sensitivity. An alternative to single-photon emitters are positron-emitters that emit two oppositely directed γ-rays after annihilation with an electron. PET has inherently higher sensitivity (up to 10-fold) and better spatial resolution than SPECT enabling lower doses of radioactivity to be used without compromising its quantitative capacity (3). In this study, we applied PET cell-imaging techniques using the long-lived PET emitter^{89}Zr (Aras, O, Berg, M, Pantin, J, Szajek, L, Paik, C, Frank, J, Sato, N, Childs, R, Choyke, P, Labeling of NK Cells with 89Zr for Positron-Emission Tomography (PET) Imaging: A New Method for in Vivo Cell Tracking. Radiological Society of North America 2012 Scientific Assembly and Annual Meeting, November 25 - November 30, 2012, Chicago IL.http://archive.rsna.org/2012/12037076.html Accessed January 8, 2015), to visualize HPCs *in vivo* that were transplanted via IB-injection. Using ^{89}Zr-labeled HPCs, we aimed to optimize the IB-HCT procedure to retain HPCs injected into BM of domestic swine, a large animal whose pelvic size and anatomy share features with humans.

Author Manuscript Author Manuscript Author Manuscript Author Manuscript

Methods

Anesthesia, monitoring, and porcine pelvis IB access

Animal procedures were approved by the institutional Animal Care and Use Committee (Study H-0233). Domestic swine (*Sus scrofa domesticus*) of both genders weighing between 38 and 70 kg were utilized. All experiments used general anesthesia; animals were sedated with ketamine, midazolam, and propofol prior to endotracheal intubation and general anesthesia was maintained with isoflurane. Analgesia was provided with local bupivacaine and IV buprenorphine. Animals had continuous EKG (Physio-Control LifePak20), end-tidal CO_2 (Ohmeda 5250 RGM), oral temperature, noninvasive pulse oximetry (NeoVet, Centaurus Medical, Saint Petersburg, FL), and intra-arterial blood pressure monitoring (ADI Powerlab with Quad Bridge Amp, ADInstruments, Colorado Springs, CO) throughout each experiment. Intravenous vecuronium was used for paralysis during imaging. Internal jugular vein and internal carotid artery cannulation were performed after cervical cut-down. A Swan-Ganz catheter (Edwards Lifesciences Corporation, Irvine, CA) was inserted via the internal jugular vein under fluoroscopic guidance, to allow continuous measuring of pulmonary artery pressures. For IB-injection, the posterior–superior iliac crest was exposed after minimal dissection. A truncated Jamshidi BM needle (Cardinal Health, Dublin, OH) with a custom threaded base was used to establish IB-access in animals for direct injection of iodinated contrast media. An OnControl™ driver (Vidacare Corp., San Antonio, TX) was used to insert modified needles having distal fenestrations (Figure 1A) for HPC IB-injections. A hemostasis screw type Y-connector (Cordis Corporation) was attached to the inserted BM needle, allowing passage of a 2Fr Millar Mikro-Tip® pressure catheter (ADInstruments) into the BM in order to provide real-time measurement of injection-pressures (Figure 1B). Intra-marrow cavity-pressure was measured continuously during IB-injection and was compared to systemic arterial pressure, pulmonary arterial pressure, and electrocardiography on a PowerLab data acquisition system (ADInstruments). Acquired hemodynamic data were analyzed using LabChart®7 (ADInstruments). At the conclusion of each experiment, animals were euthanized under anesthesia with intravenous KCl.

Porcine pelvic vascular imaging and hemodynamic monitoring

To evaluate flow through the iliac-BM, abdominal vessels were identified using iopamidol-370 contrast injected into the distal abdominal aorta with a 5Fr Glidecath (Terumo Medical Corporation, Somerset, NJ) inserted via the internal carotid artery. To evaluate the anatomy of the veins, iopamidol-370 contrast was IB-injected under anesthesia (boluses of 5 or 10mL at rates of 0.1–2.5 mL/s) while scanning with 320-row detector CT (Aquilion ONE™, Toshiba Medical, Tustin, CA). Pulmonary artery, carotid artery and intra-marrow pressures were monitored and recorded continuously both during and after injection of contrast media and HPCs. In select animals, vascular occluders (In Vivo Metric, Healdsburg, CA) were placed around the terminal branches of the abdominal aorta to selectively control flow through the internal or external iliac arteries, and around the iliac veins to control venous drainage from the pelvis. Selective catheterization of internal or external iliac arteries, with selective vessel occlusion, was performed to determine the dominant vessels supplying blood to the iliac-BM.

Author Manuscript Author Manuscript Author Manuscript Author Manuscript

Cell-labeling

HPCs utilized in all experiments had been collected by apheresis from healthy human subjects following 5 days of daily G-CSF and one dose of plerixafor after informed consent and enrollment on a National Heart Lung and Blood Institute Institutional Review Board approved protocol (ClinicalTrials.gov Identifier: NCT00082329), then were CD133+ (4) selected using the Miltenyi CliniMacs system and were cryopreserved viably.

Zr was obtained from the local cyclotron facility utilizing the nuclear reaction Y (p, 2n) ^{89}Zr and an in-house GE PETtrace™ beam-line (GE Healthcare, Chalfont St. Giles, United Kingdom) as described previously (Sato et al submitted). ^{89}Zr was provided in 1 M oxalic acid in greater than 96% radiochemical yield. Prior to cell-labeling, ^{89}Zr-oxalate was neutralized with 2 M sodium bicarbonate and 4-(2-hydroxyethyl)piperazine-1-ethanesulfonic acid, then adjusted to 1 mL by water.^{89}Zr cell-labeling was performed as previously described (Sato et al submitted). Briefly, frozen HPCs were thawed and incubated in the mixture of neutralized ^{89}Zr (0.05–0.1mCi), protamine (40 μg/mL), and heparin (2 IU/mL) in phosphate-buffered saline (PBS) for 30 min at 37°C. The cells were washed with PBS twice and then with reconstituted Df (Desferal®, Novartis Pharmaceuticals, Basel, Switzerland) in PBS in order to remove the unbound ^{89}Zr. The amount of cellular radioactivity before and after the labeling procedure was routinely determined with a *WIZARD*2 automatic γ-counter (Perkin Elmer, Waltham, MA) and dose calibrator (Capintec, Ramsey, NJ). Cell viability was assessed immediately after the labeling procedure using trypan blue then cells were injected immediately into animals. In one experiment, cell survival after labeling with ^{89}Zr was assessed *in vitro* for up to 14 h.

To determine the retention of radioisotope within the HPCs, 1×10^6 ^{89}Zr labeled human CD133+ cells (^{89}Zr-hCD133+) were cultured in RPMI medium and ^{89}Zr-activity in cells and medium was counted by a γ-counter at various time-points after labeling.

HPC IB-injection and in vivo PET/CT imaging

To evaluate the *in vivo* distribution of non-cell associated ^{89}Zr, ^{89}Zr-Df chelate (1 mCi in 10mL solution) was IV-injected into pigs followed immediately by PET/CT imaging. To determine the *in vivo* distribution of human HPCs, all animals received 2×10^8 ^{89}Zr-hCD133+ in 10mL normal saline (8–1 μCi total radioactivity) which was injected either IV into the internal jugular vein, IB into the swine iliac crest, or intra-arterially by selective catheterization of the internal iliac artery, followed by PET/CT imaging. Animals were heparinized to an ACT of 300 s or greater and received a Df IV-infusion (5 mg/kg/h) to chelate any free^{89}Zr that may have been released from any fragmented or dead cells.

Hand-injections of ^{89}Zr-hCD133+ into pigs were delivered using the minimal force needed to advance the plunger. For the non-hand-injection cohorts, IB-injections were delivered at a controlled-infusion rate of 0.2 mL/min using a Harvard PHD 22/2000 Advance Syringe Pump (Harvard Apparatus, Holliston, MA).

PET scans were performed using a Gemini TF clinical PET/CT scanner (Philips Healthcare, Andover, MA). Following injection, animals were imaged in 3D time-of-flight mode with a spatial resolution of 4.8mm at the center of the field of view. Images were reconstructed

Author Manuscript Author Manuscript Author Manuscript Author Manuscript

using the default row-action maximum-likelihood algorithm iterative reconstruction, with standard corrections for random, scatter, attenuation, and normalization.

Image analysis

Three VOIs were manually drawn within the swine PET/CT scans following capture: one VOI enclosing the iliac-BM volume near the injection-site (2) another VOI enclosing the lung volume (3) and a final VOI enclosing areas outside the iliac-BM and lung volumes. The sum of measured activities of the three volumes estimates the total injected radioactivity into the swine. The %ID within each VOI was assessed by dividing each VOI by the sum of the three VOIs × 100.

Results

Porcine pelvic vascular supply and drainage following IB-injection

Utilizing selective catheterization and 3D CT angiography, the porcine iliac-BM vascular supply and drainage following IB-injection was determined. The porcine external and internal iliac arteries arise as terminal branches of the abdominal aorta rather than from a common iliac trunk (Figure S1) however, the distribution to the pelvis is similar to humans. Blood perfusion to the iliac-BM is supplied by the internal iliac artery. Venous drainage of the iliac-BM occurs via short veins that eventually drain into a common iliac vein. Following IB-injection, contrast was observed to move first into the iliac-BM followed by opacification of short pelvic veins then the common iliac vein (Video S1). When the common iliac vein was occluded, contrast drainage from the iliac-BM occurred via veins along the iliac crest into the lumbar venous plexus, and via crosspelvic collaterals (and also via uterine veins in female pigs) to the contralateral common iliac vein.

Contrast IB-injection into the BM at rates exceeding 0.2 mL/s, volumes >10mL and IB-injections performed by hand, all resulted in contrast leakage at the site of injection outside the iliac-BM. When more than one IB access site was made in the ipsilateral iliac crest, contrast was observed to egress from the non-injected site regardless of the infusion rate and the distance between the two sites (Figure S2 and Video S2).

Hemodynamic changes during IB-injection

Reducing injection-volumes and slowing the injection-rate both reduced intra-marrow pressures following IB-injection. In particular, by not exceeding injection-rates faster than 0.2 mL/s or injection-volumes of>10 mL, intra-marrow pressures typically increased only slightly above systemic arterial pressures and were accompanied by a minimal increase in post-injection peak pulmonary artery systolic pressures (PASP) (Table 1). However, larger injection-volumes and more rapid injection-rates were associated with markedly elevated intra-marrow pressures and substantial increases in post-injection PASP (Table 1 and Figure 2). At larger volumes and more rapid injection-rates, the change in post-injection PASP appeared to decrease over time, however because increasing volume and rate injections were performed sequentially in each animal, baseline PASP remained elevated whenever injections exceeding rates of 1 mL/s were performed resulting in lower net difference. After high-volume/high-rate IB-injections, all animals developed systemic hypotension,

Author Manuscript Author Manuscript Author Manuscript Author Manuscript

tachycardia, hypoxemia and increased PASP suggesting pulmonary embolism had occurred. The occurrence of pulmonary embolism was confirmed in several swine developing these physiologic findings by subsequent CT or fluoroscopic angiography (data not shown).

Cell-labeling

Thawed hCD133+ cells were labeled with ^{89}Zr up to 7.68 μCi/million cells. At this dose, *in vitro* studies showed the majority of hCD133+ cells remained viable 14 h after labeling, establishing that the labeling process did not affect hCD133+ cell survival *in vivo*. Gradual release of ^{89}Zr from labeled-cells was observed to occur over time (Figure 3), which could protect labeled-cells *in vivo* from potentially detrimental effects of protracted radiation exposure.

Injection of ^{89}Zr-Df IV or IB

Following IV- or IB-injection of ^{89}Zr-Df (non-cell bound chelate), measurements were obtained of the radioactivity in and external to the iliac-BM, and lungs including the VOI maximum and mean pixel-value, VOI in milliliter, totalradioactivity in counts, and %ID after the first hour. One hour following IV or IB ^{89}Zr-Df administration without cells, the agent was largely confined to the blood pool, renal collecting system, ureters and bladder with little or no lung radioactivity observed. In the case of IB-injections, some radioactivity was observed to remain at the site of injection (33.5%ID) (Figure 4A and Table 2). There was no retention of ^{89}Zr in the lungs when ^{89}Zr-Df without cells was administered.

Injection of ^{89}Zr-hCD133+ cells IV and IB

In contrast to ^{89}Zr-Df administration without cells, nearly all of the radioactivity (99.7%ID) was retained in the lungs following ^{89}Zr-hCD133+ cell IV-infusions, consistent with cell trapping within the alveolar capillaries (Figure 4B and Table 2).

After selective internal iliac artery ^{89}Zr-hCD133+ cell infusion (n=1), radioactivity remained in the iliac-BM for up to 1 h; thereafter radioactivity was observed to advance in the direction of arterial flow beyond the iliac-BM (Supplementary Figure S3) and did not remain completely confined to the marrow.

One hour following ^{89}Zr-hCD133+ cell hand IB-injection into two sites on the ipsilateral iliac bone, a significant proportion of radioactivity was observed in the lungs (44.7%ID) and locally in the surrounding muscle and soft tissue outside the iliac-BM, suggesting leakage into the venous circulation with lung trapping as well as cellular extravasation from the iliac-BM (37.4%ID) (Figure 4C).

Following ^{89}Zr-hCD133+ cell hand IB-injection via a single IB site, all animals (n=3) demonstrated some retention of radioactivity in the iliac-BM, although radioactivity was readily detected within the lungs (52.2–88.2%ID) consistent with rapid leakage into the circulation with cellular-retention in the lungs (Table 2 and Figure 4D). As similarly observed with high-rate IB-injection of contrast, hand-injection of ^{89}Zr-hCD133+ cells generated extremely high intra-marrow pressures that were substantially higher than those observed with rate-controlled slow IB-infusion (0.2 mL/min) (Figure 5).

Author Manuscript Author Manuscript Author Manuscript Author Manuscript

Remarkably, when the rate of ^{89}Zr-hCD133+ cell IB-injection was decreased to 0.2 mL/min at a single IB site, radioactivity at 1 h remained completely confined to the iliac-BM (82.3–99.3%ID) without any lung radioactivity being observed (n=6) (Figure 4E and Table 2), consistent with injected-cells being retained within the marrow cavity.

Discussion

Allogeneic HCT cures many malignant and non-malignant hematological conditions. Traditionally, allogeneic HPCs are IV-infused into the recipient. For donor-engraftment to occur, HPCs must migrate or home to the BM niche utilizing cytokine gradients and their endothelial cell adhesion molecules to attach to BM endothelium, with subsequent transmigration into the extracellular space where survival and proliferation signals are received (5). Although this process leads to donor-engraftment in the majority of transplants, HPCs must overcome considerable hurdles to survive and eventually engraft including the pulmonary first-pass effect, whereby the majority of administered HPCs are initially trapped in the pulmonary vasculature (6). While not a major impediment to allogeneic BM or mobilized blood stem-cell transplants where large numbers of HPCs are infused, this maybe indeed impede engraftment when limited numbers of HPCs are transplanted, such as when umbilical cord blood (UCB) transplants are utilized. In this setting, the minimal threshold CD34+ UCB cell-dose for successful engraftment is 1.5–1.7×10^5 cells/kg recipient weight (7), which is more than one log less than the average transplanted dose of 5×10^6 CD34+ cell/kg in patients receiving mobilized allografts. This lower cell-dose is the primary factor contributing to delayed donor-engraftment and the high incidence of graft-failure associated with UCB transplantation, both which increase mortality and limit the wider applicability of this transplant approach. This limitation has led investigators to employ the use of double UCB units in adult recipients of HCT (8,9) as well as explore methods to expand *ex vivo* cord blood HPCs prior to their transplantation (10,11). Furthermore, UCB HPCs have recently been shown to have an inherently decreased homing efficiency compared to their adult counterparts, owing to a variety of factors including, but not limited to, reduced fucosylation of surface CD44 (12). While *ex vivo* fucosylation of UCB may improve engraftment (13), utilizing a mechanical approach to retain HPCs in the marrow by direct IB delivery overcomes the need for *ex vivo* incubation and manipulation of thawed UCB HPCs.

An alternative strategy to improve the success of HCT procedures that utilize low numbers of transplanted HPCs involves bypassing the pulmonary first-pass attrition effect by directly injecting donor HPCs into the recipient BM. Although the application of IB-HCT has thus far been limited to only a few investigational UCB transplant trials in humans, the current prevailing technique for IB-injection involves propofol anesthesia followed by “hand-push” injection of 5mL aliquots through a standard 14 gauge Jamshidi needle into two separate sites on the iliac-crest, repeated bilaterally for a total infused volume of 20mL (14). Our results clearly show that multiple punctures in the iliac bone lead to cellular leakage into pelvic soft tissues upon the second ipsilateral injection, potentially negating the benefits of using a direct IB-injection approach to facilitate engraftment. Despite the use of a less than optimal IB-HCT approach, clinically successful engraftment has nevertheless already been reported in humans. More than half a century ago, the first reported case of successful

Author Manuscript Author Manuscript Author Manuscript Author Manuscript

allogeneic BM transplantation to cure BM failure employed directinjection of donor BM into the recipient's sternum (15). More recently, Frassoni et al (14) and subsequently Okada et al (16) demonstrated successful engraftment in adult recipients of a single IB-transplanted UCB. However, a clinically meaningful improvement in the time to donor neutrophil engraftment compared to UCB HCT using a conventional IV approach was not clearly established by either investigator. Other attempts at IB-HCT employing larger volumes of transplanted cells did not demonstrate any advantages compared to a conventional IV approach (17,18). Hagglund et al reported no difference in outcomes between the IV- and IB-route in allogeneic BM transplantation. In their analysis, ^{99m}Tc labeled BM cells IBinfused in a volume of approximately 1000mL resulted in radioactivity identified immediately in the heart following injection (18). Brunstein et al (17) also reported no advantage for UCB-HCT using the IB-route in terms of achieving unit dominance compared to the IV-route in the setting of a double-UCB transplant.

In contrast to small-animal studies, these pilot trials in humans failed to demonstrate superior engraftment utilizing the IB-route of HCT (19-21). Xenotransplantation of human UCB HPCs into mice utilizing direct IB-injection achieves superior long-term engraftment and the ability for secondary SCID mouse repopulation (22-24). These preclinical small-animal models cannot predict engraftment kinetics in humans undergoing IB-HCT. BM blood-flow, cardiovascular physiology and anatomical size are not comparable between mouse and man. In humans, the IB-route of crystalloid infusion can rapidly restore circulating volume and blood pressure in the setting of hypovolemic shock. In fact, in large-mammal models, it has been shown that IB-infusion of crystalloid can achieve peripheral-to-central circulation times comparable to those achieved by the IV-route (25,26). Additionally, there is a substantial risk of fat-embolism following rapid IB-infusions (27,28).

We selected the porcine model used in this study because of its comparable marrow blood flow, cardiovascular physiology and pelvic anatomical size to humans (29). Using radiolabeled HPCs, we tracked injected-cells *in vivo* and optimized conditions for retaining HPCs in the BM using the IB-route. These experiments required purified HPCs to demonstrate proof of principle that the mechanical refinement of this IB infusion technique will result in retention of human HPCs in marrow. We chose to utilize purified human HPCs which were available in large numbers for these experiments, given the homology between receptor ligands expressed on human and porcine endothelial cells for their cognate receptors expressed on human HPCs (30) that allows human HPCs to traffic across porcine endothelium into swine bone marrow (31). Although investigators have shown that 5–15% of labels used for cells can be incorporated into host macrophages (32), macrophage engulfment in the first hour likely did not confound these experiments as it would have been below the threshold for radioactivity detection.

Here we demonstrate a purely mechanical method to improve the retention of HPCs in the marrow following an optimized IB delivery technique. Furthermore, we developed and optimized a novel cell-labeling technique using ^{89}Zr and protamine that is readily applicable for clinical trials that incorporate cell tracking of transplanted human HPCs. Using ^{89}Zr cell-labeling, we compared cellular-retention in the BM with different IB-injection techniques utilizing a PET/CT scanner. IV-injection of ^{89}Zr-Df alone revealed rapid renal excretion

Author Manuscript Author Manuscript Author Manuscript Author Manuscript

whereas with IV-injection of ^{89}Zr-labeled HPCs revealed extensive early lung trapping. To maximize IB-retention, we optimized the injection needle to deliver cells at right angles to the long axis using side fenestrations. By measuring injection-pressures continuously, by limiting injected-volumes and flow-rates, and by monitoring the distribution of injected-cells, we were able to determine optimal injection parameters that resulted in maximum retention of HPCs in the iliac-BM. We demonstrated that high intra-marrow pressures led to extravasation into surrounding soft tissues outside the iliac-BM and rapid venous drainage from the marrow, both sequelae that are undesirable for IB cell retention. High intra-marrow pressures also elevated PASP, likely as a consequence of procedure-associated pulmonary embolisms. While this complication has not yet been reported in current human clinical trials involving IB HCT, it does not exclude the possibility that subclinical pulmonary embolisms may have occurred. We also found that when two insertions were made into the ipsilateral iliac crest, the second injection often leaked through the first injection-site regardless of pressure or distance between the sites. Thus, we demonstrate that the maximum proportion of injected-HPCs retained in the marrow can be achieved when injection-pressures are controlled using a pump that limits the flow-rate to ≤0.2mL/min and the injected-volume to 10 mL into a single ipsilateral-site in the iliac crest. In clinical application, this will allow for 20 mL of cellular product to be split into two aliquots for infusion into both iliac crests, each through a single site. The infusion time on either side will be less than an hour, well within the time period before noticeable loss of CD34+ cell viability is observed with washed or unwashed products (33). This technique offsets limitations related to hand cell-injection where high-flow rates from the syringe into the marrow result in turbulent flow, dissipation of energy and shear-stress on the HPC cell-membrane, all which contribute to cell disruption and viability loss (34).

The successful ^{89}Zr-labeling of HPCs was pivotal in this study for monitoring their fate following injection. This method utilized a very simple mixture of ^{89}Zr and protamine with cells. As cellular uptake of the ^{89}Zr-protamine complex was self-limited, only miniscule doses of radioactivity (approximately 10 μCi per 2×10^8 hCD133+ cells) was retained by the cells, preserving a high viability among labeled-cells with little chance of cell-death occurring from radiation effects. In fact, the viability of the labeled-cells at 14 h was comparable to unlabeled-cells in a single experiment. Our unpublished data of long-term effects of labeling with ^{89}Zr in other mononuclear cell populations suggests that the phenotype and function of cells are unaffected by the labeling process. The ability to accurately detect and image with such a low dose of radioactivity greatly reduces the risk of time-dependent cytotoxicity seen with the larger doses of ^{111}In-oxine required for cell-labeling (1). The sensitivity of PET/CT scanners enables detection of this small dose of cellular radioactivity. ^{89}Zr has several advantages for this task: it has a sufficiently long half-life (78.4 h) to track cells for up to a week and its physical properties produce relatively high spatial resolution (35) compared to other positron emitters. Because PET cameras are highly sensitive and have relatively better resolution than SPECT cameras and because there is no background signal in the recipient, even very tiny amounts of radioactivity can be detected. Moreover, since PET images are superimposed on high-resolution CT images, it is possible to accurately localize the injected-cells with a high degree of certainty.

Author Manuscript Author Manuscript Author Manuscript Author Manuscript

This study was not designed to demonstrate that confining transferred HPCs to the BM results in improved engraftment following HCT. However, our data does support a methodology of HPC labeling that can be used to optimize, standardize and validate IB-injection in humans, removing uncertainty and inconsistency in cellular-delivery methods for patients undergoing this investigational transplant approach. Human clinical trials are required to demonstrate whether this optimized IB-transplantation method reported results in superior donor-engraftment in humans undergoing UCB HCT. In a syngeneic mouse model, engraftment and hematopoietic reconstitution levels were very similar between IB- and IV-transplanted mice (36). However, in congenic HPC transplantation in rats although IB-injection resulted in rapid delivery to the bloodstream, there still was reduced pulmonary sequestration compared with IV-injected HPCs, suggesting that first-contact with the BM resulted in improved recruitment back to their hematopoietic niche (37).

There may be other advantages to utilizing an IB-approach to transplantation. In the largest human clinical trial of UCB IB-HCT in acute leukemia, none of the 26 evaluable patients developed grade III–IV acute-GVHD. This is in contrast to the 9% risk of severe acute-GVHD reported in other UCB HCT clinical trials (38,39). Although antithymocyte globulin was used in the preparative regimen and could have contributed to the lower incidence of acute-GVHD compared to conventional UCB HCT, this immunological advantage was also demonstrated in small-mammal models of IB-HCT. In a mismatched murine model of allogeneic HCT where C57BL/6 recipient mice received BALB/c donor BM and lymphocytes either IB or IV, the IB route was associated with an abrogation of GVHD (40). Similarly, in a rabbit model of haploidentical HCT, engraftment was improved and GVHD reduced in IB compared to IV transplant recipients (41). In another study, Brown Norway rats were the recipients of hind limbs transplanted from donor Fischer 344 rats together with an IB transplant of donor bone marrow cells after fludarabine and low dose irradiation conditioning. Recipients achieved complete donor lympho-hematopoietic engraftment and transplanted limbs were accepted for more than 1 year without any clinical signs of rejection. Lymphocytes harvested from transplanted recipient rats showed tolerance to both donortype and recipient-type major histocompatibility complex determinants in mixed lymphocyte reaction assays but maintained a preserved response against third party (42). Thus, optimized IB-HCT in humans could offer multiple immunological advantages in addition to the potential of improving engraftment in the context of transplants that utilize small number of donor HPCs or for induction of tolerance in recipients of combined bone marrow solid organ transplants.

In summary, we show that conventional methods utilized for IB-HCT in humans are ineffective in maintaining cells in the marrow space. Utilizing a novel cell-labeling technique, we developed a method to optimize the retention of HPCs in the BM, which was contingent upon real-time intra-marrow pressure monitoring and reducing the infusion rate and volume. A key component to the success of this technique was the use of a modified needle with side fenestrations allowing for real-time continuous monitoring of intra-marrow pressures during IB-injection, as maintaining low IB-pressures was found to be essential to retain cells within the marrow. The development of a device that uses continuous pressure feedback monitoring to regulate the infusion rate to maintain low intra-marrow pressure is key to this work and will need further testing to determine if the maximum volume of

Author Manuscript Author Manuscript Author Manuscript Author Manuscript

cells that can be delivered varies depending on patient specific variables such as pelvic size and/or the specific location where IB delivery of cells occurs. The injection methods used in this study have establish an optimized technique that is currently being used to investigate the impact of IB-HCT on engraftment in a non-human primate model, and further lays the foundation for future clinical trials that systematically explore IB-HCT in humans.

Supplementary Material

Refer to Web version on PubMed Central for supplementary material.

Acknowledgments

This work was supported by the Division of Intramural Research (DIR) of the NHLBI and the NCI. Peter Herscovitch, M.D., Dale Kiesewetter, Ph.D., Chang Paik Ph.D., Eric Munger, Karen Wong, Karen Keeran, Gayle Nugent, Arthur Zetts, Kenneth Jeffries, Shawn Kozlov, Gideon Kwarteng, Lawrence Szajek, Ph.D., Joseph Frank, M.D., M.S., Thomas Philbeck, Ph.D., and Hahn Khuu, M.D., were all instrumental in the completion of this project.

Abbreviations:

%ID	percent-injected dose
3D	3-dimensional
ACT	activated clotting time
BM	bone marrow
CD	cluster differentiation
Ci	Curie
CT	computed tomography
Df	deferoxamine
Fr	French
G-CSF	granulocyte-colony stimulating factor
GVHD	graft-versus-host disease
hCD133+	human CD133 positive
HCT	hematopoietic cell transplantation
HPC	hematopoietic progenitor cell
IB	intrabone
In	indium
IV	intravenous
KCI	potassium chloride

Author Manuscript Author Manuscript Author Manuscript Author Manuscript

M	molar
MSC	mesenchymal stromal cell
PASP	pulmonary artery systolic pressure
PBS	phosphate buffered saline
PET	positron emission tomography
SCID	severe combined immunodeficiency
SPECT	single-photon emission computed tomography
Tc	rechnetium sestamibi
UCB	umbilical cord blood
VOI	volume of interest
Y	Yttrium
Zr	Zirconium

References

1. Gholamrezanezhad A, Mirpour S, Bagheri M, Malekzadeh R, Saghari M. Cytotoxicity of 111In-oxine on mesenchymal stem cells: A time dependent effect. Eur J Nucl Med Mol Imaging2008; 35: S317–S317.
2. Gildehaus FJ, Haasters F, Drosse I, et al.Impact of indium-111 oxine labelling on viability of human mesenchymal stem cells in vitro, and 3D cell-tracking using SPECT/CT in vivo. Mol Imaging Biol2011; 13: 1204–1214. [PubMed: 21080231]
3. Rahmim A, Zaidi H. PET versus SPECT: Strengths, limitations and challenges. Nucl Med Commun2008; 29: 193–207. [PubMed: 18349789]
4. Yin AH, Miraglia S, Zanjani ED, et al.AC133, a novel marker for human hematopoietic stem and progenitor cells. Blood1997; 90: 5002–5012. [PubMed: 9389720]
5. Lapidot T, Dar A, Kollet O. How do stem cells find their way home?Blood2005; 106: 1901–1910. [PubMed: 15890683]
6. Fischer UM, Harting MT, Jimenez F, et al.Pulmonary passage is a major obstacle for intravenous stem cell delivery: The pulmonary first-pass effect. Stem Cells Dev2009; 18: 683–691. [PubMed: 19099374]
7. Wagner JE, Barker JN, DeFor TE, et al.Transplantation of unrelated donor umbilical cord blood in 102 patients with malignant and nonmalignant diseases: Influence of CD34 cell dose and HLA disparity on treatment-related mortality and survival. Blood2002; 100: 1611–1618. [PubMed: 12176879]
8. Barker JN, Weisdorf DJ, DeFor TE, et al.Transplantation of 2 partially HLA-matched umbilical cord blood units to enhance engraftment in adults with hematologic malignancy. Blood2005; 105: 1343–1347. [PubMed: 15466923]
9. Rocha V, Crotta A, Ruggeri A, et al.Double cord blood transplantation: Extending the use of unrelated umbilical cord blood cells for patients with hematological diseases. Best Pract Res Clin Haematol2010; 23: 223–229. [PubMed: 20837334]
10. Delaney C, Heimfeld S, Brashem-Stein C, Voorhies H, Manger RL, Bernstein ID. Notch-mediated expansion of human cord blood progenitor cells capable of rapid myeloid reconstitution. Nat Med2010; 16: 232–236. [PubMed: 20081862]

Author Manuscript Author Manuscript Author Manuscript Author Manuscript

11. Duchez P, Chevaleyre J, Vlaski M, et al.Definitive setup of clinical scale procedure for ex vivo expansion of cord blood hematopoietic cells for transplantation. Cell Transplant2012; 21: 2517–2521. [PubMed: 22469365]
12. Xia LJ, McDaniel JM, Yago T, Doeden A, McEver RP. Surface fucosylation of human cord blood cells augments binding to P-selectin and E-selectin and enhances engraftment in bone marrow. Blood2004; 104: 3091–3096. [PubMed: 15280192]
13. Robinson SN, Thomas MW, Simmons PJ, et al.Fucosylation with fucosyltransferase VI or fucosyltransferase VII improves cord blood engraftment. Cytotherapy2014; 16: 84–89. [PubMed: 24094497]
14. Frassoni F, Gualandi F, Podesta M, et al.Direct intrabone transplant of unrelated cord-blood cells in acute leukaemia: A phase I/II study. Lancet Oncol2008; 9: 831–839. [PubMed: 18693069]
15. Morrison M, Samwick AA. Intramedullary (sternal) transfusion of human bone marrow: Preliminary report. J Am Med Assoc1940; 115: 1708–1711.
16. Okada M, Yoshihara S, Taniguchi K, et al.Intrabone marrow transplantation of unwashed cord blood using reduced-intensity conditioning treatment: A phase I study. Biol Blood Marrow Transplant2012; 18: 633–639. [PubMed: 21867667]
17. Brunstein CG, Barker JN, Weisdorf DJ, et al.Intra-BM injection to enhance engraftment after myeloablative umbilical cord blood transplantation with two partially HLA-matched units. Bone Marrow Transpl2009; 43: 935–940.
18. Hagglund H, Ringden O, Agren B, et al.Intraosseous compared to intravenous infusion of allogeneic bone marrow. Bone Marrow Transpl1998; 21: 331–335.
19. Li Q, Hisha H, Yasumizu R, et al.Analyses of very early hemopoietic regeneration after bone marrow transplantation: Comparison of intravenous and intrabone marrow routes. Stem Cells2007; 25: 1186–1194. [PubMed: 17322105]
20. Mazurier F, Doedens M, Gan OI, Dick JE. Rapid myeloerythroid repopulation after intrafemoral transplantation of NOD-SCID mice reveals a new class of human stem cells. Nat Med2003; 9: 959–963. [PubMed: 12796774]
21. Omae M, Inaba M, Sakaguchi Y, et al.Long-term maintenance of donor-derived hematopoiesis by intra-bone marrow-bone marrow transplantation. Stem Cells Dev2008; 17: 291–302. [PubMed: 18447644]
22. Wang JF, Kimura T, Asada R, et al.SCID-repopulating cell activity of human cord blood-derived CD34(−) cells assured by intra-bone marrow injection. Blood2003; 101: 2924–2931. [PubMed: 12480697]
23. Kimura T, Matsuoka Y, Murakami M, et al.In vivo dynamics of human cord blood-derived CD34(−) SCID-repopulating cells using intra-bone marrow injection. Leukemia2010; 24: 162–168. [PubMed: 19798093]
24. Yahata T, Ando K, Sato T, et al.A highly sensitive strategy for SCID-repopulating cell assay by direct injection of primitive human hematopoietic cells into NOD/SCID mice bone marrow. Blood2003; 101: 2905–2913. [PubMed: 12411299]
25. Cameron JL, Fontanarosa PB, Passalaqua AM. A comparative study of peripheral to central circulation delivery times between intraosseous and intravenous injection using a radionuclide technique in normovolemic and hypovolemic canines. J Emerg Med1989; 7: 123–127. [PubMed: 2738371]
26. Schoffstall JM, Spivey WH, Davidheiser S, Lathers CM. Intraosseous crystalloid and blood infusion in a swine model. J Trauma1989; 29: 384–387. [PubMed: 2926854]
27. Hasan MY, Kissoon N, Fiallos M, Abdelmoneim T, Johnson L, Murphy S. Incidence of fat and bone marrow embolism with the use of intraosseous infusion during cardio-pulmonary resuscitation. Pediatrics1997; 100: 455–455.
28. Orlowski JP, Julius CJ, Petras RE, Porembka DT, Gallagher JM. The safety of intraosseous infusions—Risks of fat and bonemarrow emboli to the lungs. Ann Emerg Med1989; 18: 1062–1068. [PubMed: 2802282]
29. Upton RN. Organ weights and blood flows of sheep and pig for physiological pharmacokinetic modelling. J Pharmacol Toxicol Methods2008; 58: 198–205. [PubMed: 18775498]

Author Manuscript Author Manuscript Author Manuscript Author Manuscript

30. Warrens AN, Simon AR, Theodore PR, Sykes M. Human-porcine receptor-ligand compatibility within the immune system: Relevance for xenotransplantation. Xenotransplantation1999; 6: 75–78. [PubMed: 10431783]

31. Fujiki Y, Fukawa K, Kameyama K, et al.Successful multilineage engraftment of human cord blood cells in pigs after in utero transplantation. Transplantation2003; 75: 916–922. [PubMed: 12698074]

32. Pawelczyk E, Jordan EK, Balakumaran A, et al.In vivo transfer of intracellular labels from locally implanted bone marrow stromal cells to resident tissue macrophages. PLoS ONE2009; 4: e6712. [PubMed: 19696933]

33. Regan DM, Wofford JD, Wall DA. Comparison of cord blood thawing methods on cell recovery, potency, and infusion. Transfusion2010; 50: 2670–2675. [PubMed: 21126251]

34. Zhang Z, Alrubeai M, Thomas CR. Estimation of disruption of animal-cells by turbulent capillary-flow. Biotechnol Bioeng1993; 42: 987–993. [PubMed: 18613147]

35. Laforest R, Liu X. Image quality with non-standard nuclides in PET. Q J NuclMed Mol Imaging2008; 52: 151–158.

36. van Os R, Ausema A, Dontje B, van Riezen M, van Dam G, de Haan G. Engraftment of syngeneic bone marrow is not more efficient after intrafemoral transplantation than after traditional intravenous administration. Exp Hematol2010; 38: 1115–1123. [PubMed: 20643182]

37. Massollo M, Podesta M, Marini C, et al.Contact with the bone marrow microenvironment readdresses the fate of transplanted hematopoietic stem cells. Exp Hematol2010; 38: 968–977. [PubMed: 20550953]

38. Thomson BG, Robertson KA, Gowan D, et al.Analysis of engraftment, graft-versus-host disease, and immune recovery following unrelated donor cord blood transplantation. Blood2000; 96: 2703–2711. [PubMed: 11023501]

39. Barker JN, Weisdorf DJ, DeFor TE, Blazar BR, Miller JS, Wagner JE. Rapid and complete donor chimerism in adult recipients of unrelated donor umbilical cord blood transplantation after reduced-intensity conditioning. Blood2003; 102: 1915–1919. [PubMed: 12738676]

40. Miyake T, Inaba M, Fukui J, et al.Prevention of graft-versus-host disease by intrabone marrow injection of donor T cells: Involvement of bone marrow stromal cells. Clin Exp Immunol2008; 152: 153–162. [PubMed: 18307515]

41. Cui Y, Nakamura S, Shi M, et al.A successful haploidentical bone marrow transplantation method in rabbits: Perfusion method plus intra-bone marrow-bone marrow transplantation. Transpl Immunol2010; 24: 33–39. [PubMed: 20624463]

42. Esumi T, Inaba M, Ichioka N, Kushida T, Iida H, Ikehara S. Successful allogeneic leg transplantation in rats in conjunction with intra-bone marrow injection of donor bone marrow cells. Transplantation2003; 76: 1543–1548. [PubMed: 14702521]

Author Manuscript Author Manuscript Author Manuscript Author Manuscript

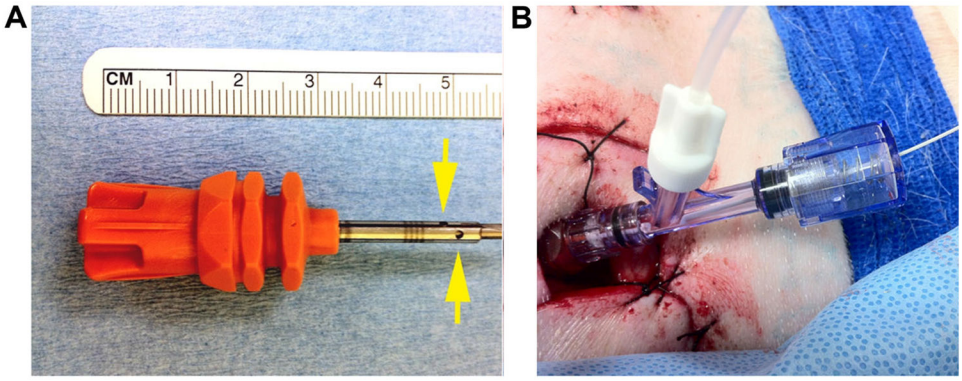

Figure 1:

(A) Shortened OnControl™ needle with distal fenestrations (arrows) added. In all experiments, this needle was driven directly into the iliac-crest to the hub. A longer needle was used for CT-guided percutaneous access. (B) Simultaneous infusion and intra-marrow pressure monitoring with a Millar catheter through a hemostasis screw type Y-connector connected to an OnControl™ needled inserted into the iliac-crest.

Author Manuscript Author Manuscript Author Manuscript Author Manuscript

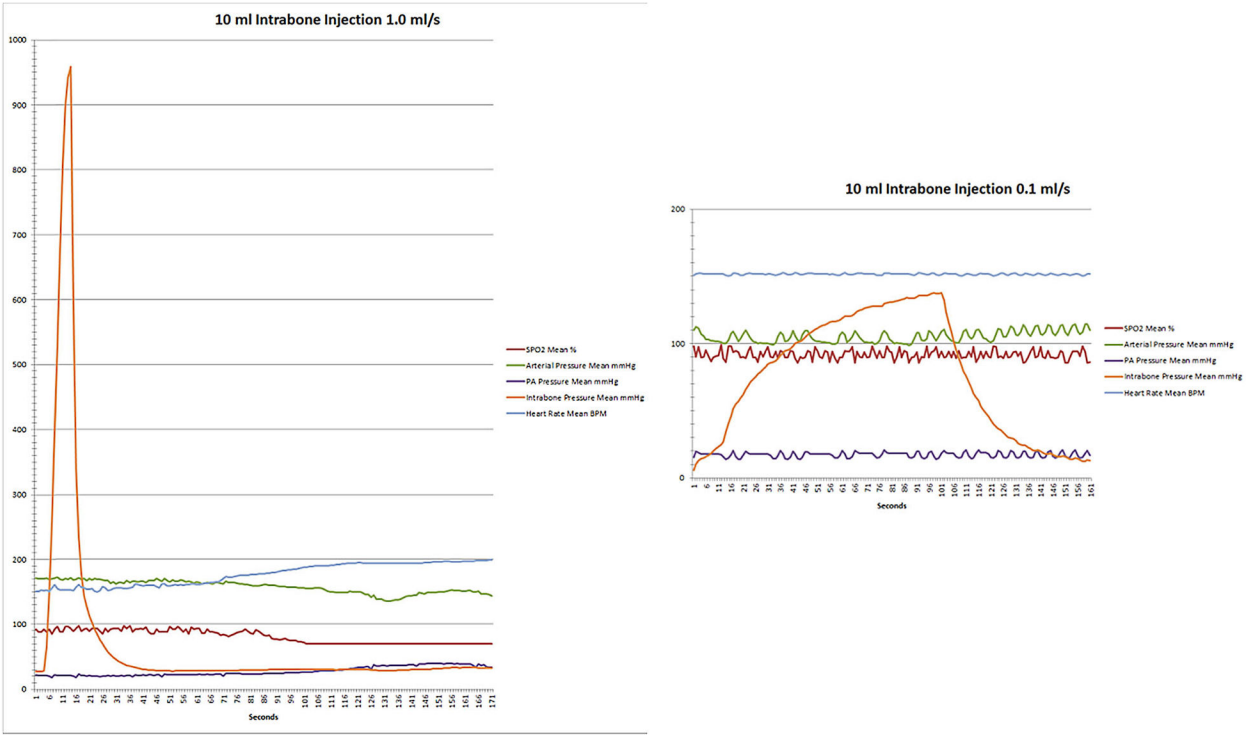

Figure 2: Physiologic parameters following IB-injection of 10 mL of iopamidol-370 contrast at 1.0 mL/s (rapid) and at 0.1 mL/s (slow) in a representative animal experiment.

With rapid injection, there was a significant peak in intra-marrow pressure followed by an increase in PA pressure, a decrease in systemic arterial pressure, and the development of tachycardia. When injection-rates were slowed, changes in these parameters were not observed.

Author Manuscript Author Manuscript Author Manuscript Author Manuscript

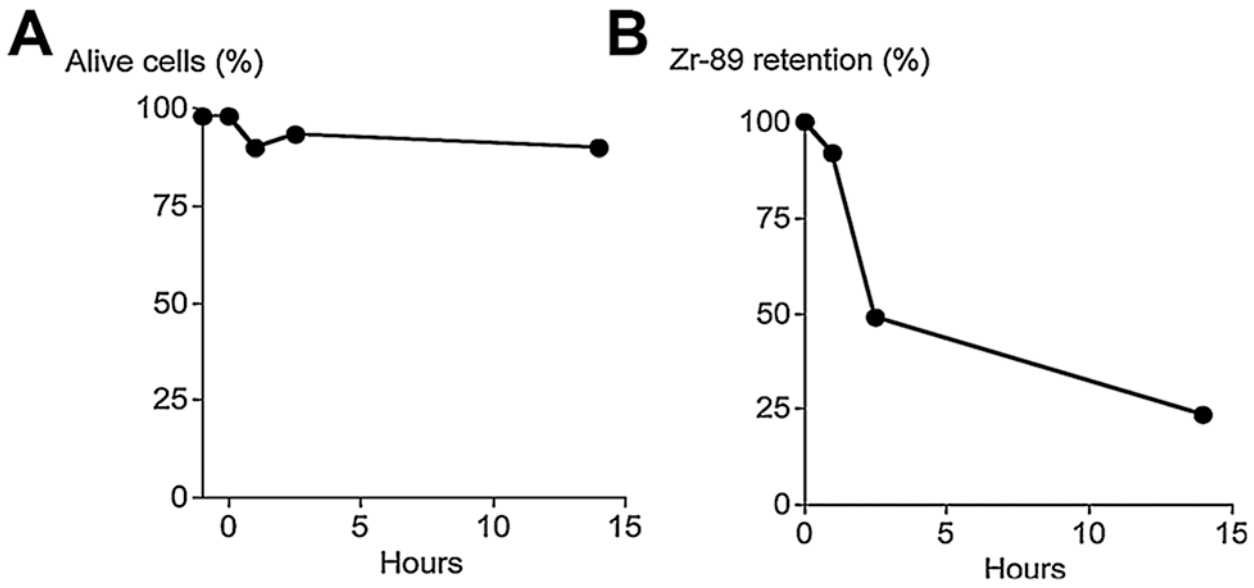

Figure 3: hCD133$_+$ cells were labeled with neutralized ^{89}Zr as described.
(A) ^{89}Zr labeling of hCD133+ cells did not affect their survival *in vivo* for up to 14 h. (B) ^{89}Zr was gradually released from ^{89}Zr-hCD133+ cells.

Author Manuscript Author Manuscript Author Manuscript Author Manuscript

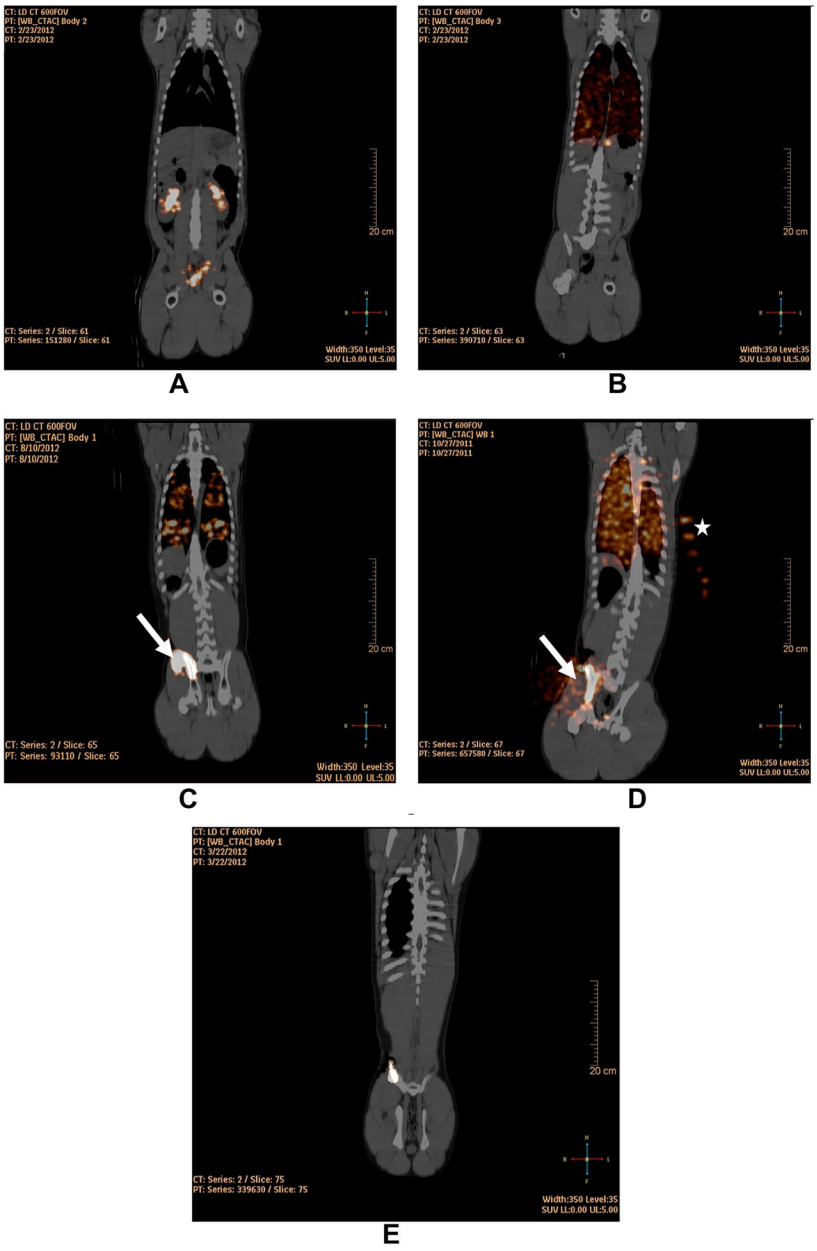

Figure 4:

Fusion PET/CT coronal images at 1 h following (A) IB-injection of ^{89}Zr-Df with radioactivity in the renal pelvises and bladder (Pig ID# 32890); (B) IV-injection of ^{89}Zr-hCD133+ with radioactivity confined to the lung (Pig ID#32891); (C) Hand IB-injection of ^{89}Zr-hCD133+ into two sites on the right iliac-crest demonstrating radioactivity leaked at the first site of injection (arrow) and radioactivity within the iliac-BM and lungs (Pig ID#34489); (D) hand IB-injection of ^{89}Zr-hCD133+ into a single site on the right iliac-crest demonstrating radioactivity leaked at the sight of injection (arrow) and radioactivity within the iliac-BM and lungs (Pig ID# 31717); (E) slow non-manual IB-infusion (0.2 mL/min) of ^{89}Zr-hCD133+ into the right iliac-crest demonstrating radioactivity confined within the

Author Manuscript Author Manuscript Author Manuscript Author Manuscript

iliac-BM (Pig ID# 33189). Note that in (D) there is radioactivity highlighted in syringes of ^{89}Zr-oxalate placed to the left of the swine for calibration and decay correction (star).

Author Manuscript Author Manuscript Author Manuscript Author Manuscript

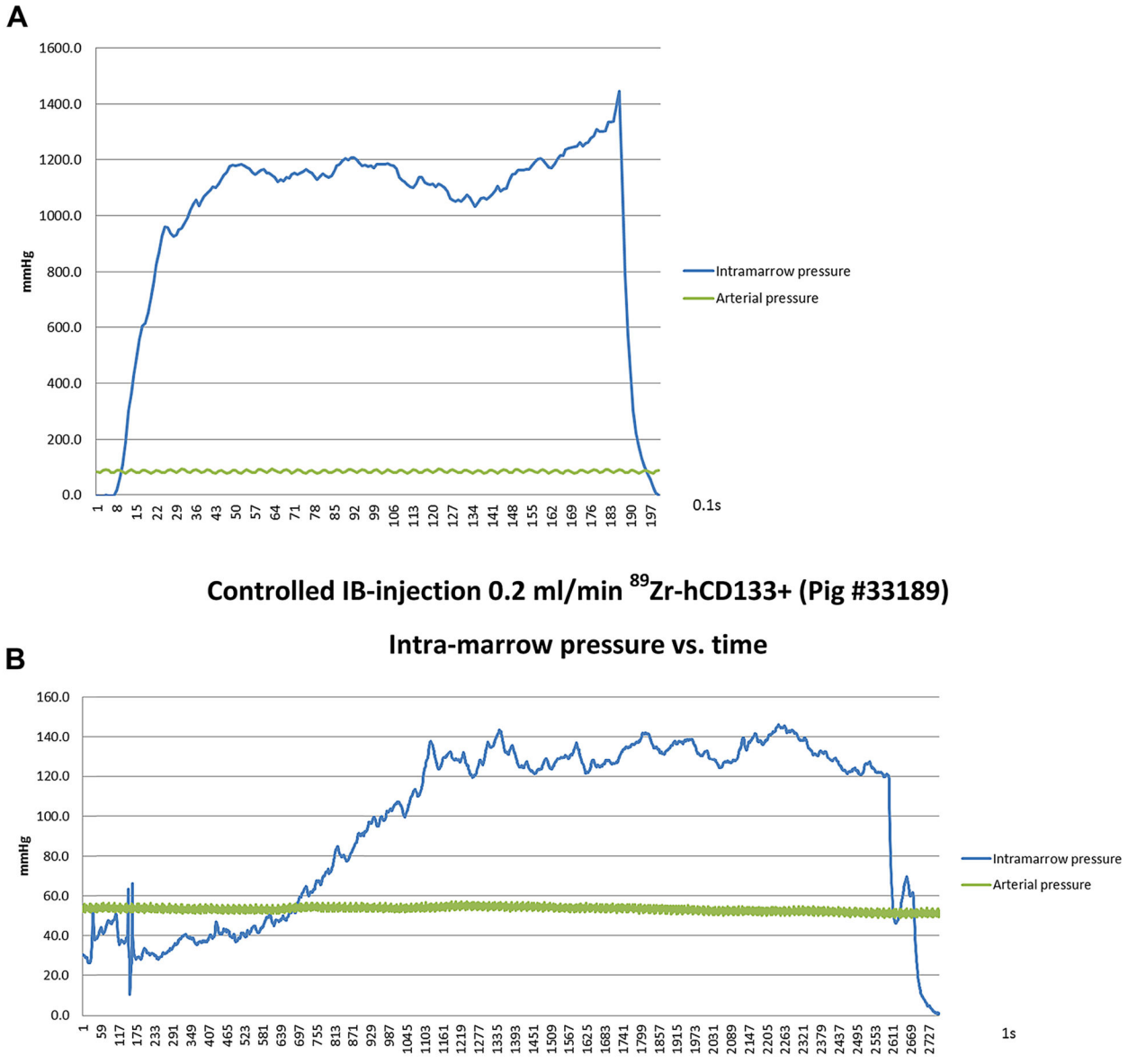

Figure 5:

Systemic arterial and intra-marrow pressures over time during (A) hand IB-injection of ^{89}Zr-hCD133+ into the iliac-crest through a single site and (B) slow controlled non-manual infusion at 0.2 mL/min of ^{89}Zr-hCD133+ into the iliac-crest through a single site.

Author Manuscript Author Manuscript Author Manuscript Author Manuscript

Table 1:

Peak intra-marrow pressure and change in pulmonary artery systolic pressure following IB-injection at varying rates and volumes

Volume injected (mL)	Rate injected (mL/s)	Number of experiments	Δ from baseline in intra-marrow pressure (mmHg), mean ± SE	Δ from baseline in peak pulmonary artery systolic pressure (PASP) (mmHg), mean ± SE
10	0.1	4	159.3 ± 57.7	1.5 ± 0.7
10	0.2	3	300.3 ± 149.3	3.5 ± 1.0
10	0.5	2	803.4 ± 483.0	13.0 ± 5.1
10	1.0	2	1196.0 ± 265.5	8.9 ± 9.3
10	2.5	3	1689.0 ± 116.0	2.2 ± 1.0
5	0.1	2	128.7 ± 60.2	−0.5 ± 0.4
5	0.2	2	256.7 ± 42.7	1.3 ± 1.3
5	0.5	1	802.9	6.1
5	1.0	1	1490.8	0
5	2.5	1	997.5	2

Am J Transplant. Author manuscript; available in PMC 2021 August 27.

Author Manuscript Author Manuscript Author Manuscript Author Manuscript

Table 2:

The region of interest (ROI) maximum and mean pixel value, ROI volume, total radioactivity in counts, and percent of injected dose (%ID) after the first hour for within the iliac marrow (intra-iliac-BM); outside the iliac-BM but within the pelvis (extra-pelvic); and in the lungs; for each pig administered ^{89}Zr-deferoxamine chelate (^{89}Zr-Df) or ^{89}Zr-radiolabeled human CD133+ cells (^{89}Zr-hCD133+) either IV or IB

Pig ID#	Weight (kg)	Injection	Group	Volume injected (mL)	Intra-iliac marrow VOI (max.)	Intra-iliac marrow VOI (mean)	Volume of intra-iliac marrow VOI (mL)	Extra-pelvic VOI (max.)	Extra-pelvic VOI (Mean)	Volume of Extra-pelvic VOI (mL)	Lung VOI (max.)	Lung VOI (mean)	Volume of lung VOI (mL)	Intra-iliac marrow total radioactivity	Extra-pelvic total radioactivity	Lung total radioactivity	Intra-iliac marrow %ID	Extra-pelvic %ID	Lung %ID
32890	52	^{89}Zr-Df	Control	10	338.9	114.42	9.49	91.45	16.32	132.26	2.39	0	2159.22	1085.85	2158.48	0	33.5%	66.5%	0.0%
32891	53	^{89}Zr-hCD133+	IV	10	0	0	0	1.98	0.17	27.82	17.21	0.38	3556.15	0	4.73	1351.34	0.0%	0.3%	99.7%
34489	43	^{89}Zr-hCD133+	IB-hand (2 ipsilateral sites)	5 (×2)	503.83	174.36	5	618.99	225.93	8.03	38.04	1.28	1693.94	871.80	1814.22	2168.24	18.0%	37.4%	44.7%
34490	43	^{89}Zr-hCD133+	IB-hand	10	1974.18	272.53	18.41	293.04	150.35	9.41	303.32	22.29	2154.72	5017.28	1414.79	48 028.71	9.2%	2.6%	88.2%
33185	47	^{89}Zr-hCD133+	IB-hand	10	98.32	16.65	9.08	15.13	5.32	3.35	10.8	0.09	3774.47	151.18	17.82	339.70	29.7%	3.5%	66.8%
31717	51	^{89}Zr-hCD133+	IB-hand	10	1114.79	231.79	8.76	223.35	113.69	27.04	24.62	1.95	2862.3	2030.48	3074.18	5581.49	19.0%	28.8%	52.2%
33186	44	^{89}Zr-hCD133+	IB-slow	10	276.65	65.92	4.13	18.21	6.53	2.16	0	0	3364.94	272.25	14.10	0	95.1%	4.9%	0.0%
33189	52	^{89}Zr-hCD133+	IB-slow	10	1685.55	244.9	6.3	47.82	15.57	1.62	0	0	2949.48	1542.87	25.22	0	98.4%	1.6%	0.0%
33190	50	^{89}Zr-hCD133+	IB-slow	10	1210.75	230.51	6.89	275.87	34.17	9.98	0	0	2466.73	1588.21	341.02	0	82.3%	17.7%	0.0%
33296	40	^{89}Zr-hCD133+	IB-slow	10	986.39	168.28	4.93	13.83	3.86	1.6	0	0	2245	829.62	6.18	0	99.3%	0.7%	0.0%
32261	48.6	^{89}Zr-hCD133+	IB-slow	10	2580.88	958.73	2.54	75.42	25.57	1.45	0	0	2120.79	2435.17	37.08	0	98.5%	1.5%	0.0%
33300	38	^{89}Zr-hCD133+	IB-slow	10	1145.85	200.71	5.11	40.77	13.41	3.31	0	0	2087.17	1025.63	44.39	0	95.9%	4.1%	0.0%

Am J Transplant. Author manuscript; available in PMC 2021 August 27.